Journal of Enzyme Inhibition and Medicinal Chemistry, 2010; 25(3): 414–420

informa
healthcare

RESEARCH ARTICLE

Nostotrebin 6, a bis(cyclopentenedione) with cholinesterase inhibitory activity isolated from *Nostoc* sp. str. Lukešová 27/97

Petr Zelík[1,7], Alena Lukešová[2], Jan Čejka[3], Miloš Buděšínský[4], Vladimír Havlíček[5], Alexander Čegan[6], and Jiří Kopecký[7]

[1]*Institute of Physical and Applied Chemistry, Faculty of Chemistry, Brno University of Technology, Brno, Czech Republic,* [2]*Institute of Soil Biology, Biology Center of the Academy of Sciences of the Czech Republic, České Budějovice, Czech Republic,* [3]*Department of Solid State Chemistry, Faculty of Chemical Technology, Institute of Chemical Technology, Prague, Czech Republic,* [4]*Institute of Organic Chemistry and Biochemistry, Academy of Sciences of the Czech Republic, Prague, Czech Republic,* [5]*Laboratory of Molecular Structure Characterization, Institute of Microbiology, Academy of Sciences of the Czech Republic, Prague, Czech Republic,* [6]*Department of Biological and Biochemical Sciences, Faculty of Chemical Technology, University of Pardubice, Pardubice, Czech Republic, and* [7]*Department of Autotrophic Microorganisms, Institute of Microbiology, Academy of Sciences of the Czech Republic, Třeboň, Czech Republic*

Abstract

Nostotrebin 6, a new polyphenolic compound with a fully substituted 2,2′-bis(cyclopent-4-en-1,3-dione) skeleton, was isolated from a methanolic extract of the cyanobacterial strain *Nostoc* sp. str. Lukešová 27/97. The structure of this compound was determined using X-ray crystallography and further supported by NMR, IR spectroscopy, and MS. Nostotrebin 6 is an *S*-parabolic *I*-parabolic noncompetitive inhibitor of acetylcholinesterase (IC_{50} = 5.5 μM) and an *S*-parabolic *I*-parabolic mixed inhibitor of butyrylcholinesterase (IC_{50} = 6.1–7.5 μM). The inhibitory potency of nostotrebin 6 was compared with that of tacrine and galanthamine.

Keywords: *Cholinesterase inhibitor; cyclopentenedione; cyanobacteria;* Nostoc*; nostotrebin 6*

Introduction

Acetylcholinesterase (AChE, EC 3.1.1.7) catalyzes the hydrolysis of the neurotransmitter acetylcholine, and thus terminates cholinergic neurotransmission. Targeted inhibition of this enzyme is currently used in the therapy of Alzheimer's disease (AD), to improve cholinergic functions through the prolongation of the cholinergic synapse, and by increasing the likelihood of a signal in the postsynaptic cholinergic neuron[1]. Nevertheless, in AD therapy, dual cholinesterase inhibitors that inhibit both AChE and butyrylcholinesterase (BChE, EC 3.1.1.8) are considered to have both better and longer therapeutic results, compared to selective AChE inhibitors[2].

The search for new cholinesterase (ChE) inhibitors still constitutes an important focus in the development of medications for Alzheimer's disease. Many of the known natural ChE inhibitors have primarily been isolated from higher plants, being the traditional source of bioactive metabolites. Algae and cyanobacteria are also a promising source for structurally new types of secondary metabolites, as well as unique biological activities; this is due to their differences in metabolism, compared to higher plants[3]. However, to date only a few algal and cyanobacterial strains have been studied for ChE inhibitors despite the increasing interest in the secondary metabolites of these microorganisms[4–9].

Based on our screening for AChE inhibitory activity in cyanobacteria and algae originating from different types of habitat and geographical areas, we have selected one of the most active cyanobacterial strains (*Nostoc* sp. str. Lukešová 27/97) for further study. The active fraction responsible for the anti-AChE activity was identified in a crude methanolic extract of *N.* sp. str. Lukešová 27/97 using high performance liquid chromatography/mass spectrometry (HPLC/MS), as a single peak (according to HPLC analysis) with the molecular ion $[M + H]^+$ *m/z* 799.4[10].

In this study, a novel AChE inhibitor, named nostotrebin 6 (Figure 1), was isolated from a crude methanolic extract of a

Address for Correspondence: Dr Petr Zelík, Institute of Physical and Applied Chemistry, Faculty of Chemistry, Brno University of Technology, Purkyňova 118, Brno, 612 00 Czech Republic. E-mail: zelikp@gmail.com.

(Received 19 May 2009; revised 21 July 2009; accepted 28 July 2009)

ISSN 1475-6366 print/ISSN 1475-6374 online © 2010 Informa UK Ltd
DOI: 10.3109/14756360903213481

Journal of Enzyme Inhibition and Medicinal Chemistry Downloaded from informahealthcare.com by University of South Carolina on 12/26/11
For personal use only.

RIGHTSLINK

Journal of Enzyme Inhibition and Medicinal Chemistry Downloaded from informahealthcare.com by University of South Carolina on 12/26/11
For personal use only.

freeze-dried biomass of *N.* sp. str. Lukešová 27/97. Its structure was determined by X-ray crystallography and verified by other structural analysis techniques nuclear magnetic resonance (NMR), infrared (IR) spectroscopy, and mass spectrometry (MS). *In vitro* biological study has shown potent inhibition of both AChE and BChE in the presence of nostotrebin 6.

Materials and methods

Chemicals

Acetylthiocholine iodide (ATCI), butyrylthiocholine iodide (BTCI), 5,5´-dithiobis(2-nitrobenzoic acid) (DTNB), AChE from the electric eel (type VI-S), BChE from equine serum, and tacrine were all obtained from Sigma-Aldrich (Czech Republic). Acetonitrile and methanol (both HPLC gradient grade) were obtained from Analytika (Czech Republic). All of the other chemicals were analytical grade.

Origin and cultivation of Nostoc sp. str. Lukešová 27/97

The *N.* sp. str. Lukešová 27/97 used was obtained from the culture collection of soil algae and cyanobacteria of the Institute of Soil Biology of the Academy of Sciences of the Czech Republic.

Cultivation was carried out in an 8.0 L glass tube containing Allen & Arnon medium[11], using a semi-batch system, at the constant temperature of 25 ± 0.5°C, with continuous illumination (351 μmol m^{-1} s^{-1}). The medium was stirred using a flow of mixed air and CO_2 (98:2; V/V). After depletion of nitrates from the cultivation medium, the biomass from four-fifths of the total cultivation medium volume was harvested by centrifugation and then lyophilized. The remaining one-fifth of the suspension was refilled with freshly prepared Allen & Arnon medium. The cultivation was repeated several times in order to get a total of 66.7 g of freeze-dried biomass of *N.* sp. str. Lukešová 27/97.

Analysis of nitrates

A Dionex ICS-90 ion chromatography system, with Chromeleon Client 6.50 SP3 Build 980 software, was used for the analysis of the nitrates. Samples of 1.5 mL of medium were centrifuged, and 10 μL of the supernatant injected onto an IonPac® AS9-HC (4×250 mm) analytical column, and then eluted with a mobile phase of 9 mM Na_2CO_3 at a flow rate of 1 mL min^{-1}. A bipolar heated conductivity cell detector was used to detect the nitrates.

Isolation of nostotrebin 6

The 66.7 g of freeze-dried biomass of *N.* sp. str. Lukešová 27/97 was homogenized with sea-sand and then extracted with 800 mL of methanol. The extraction procedure was then further repeated with 530 mL of methanol, three times. The combined methanolic extracts were evaporated until dry, the resulting residue was dissolved in 30 mL of acetone, and then 600 mL of hexane was added. The precipitate obtained was separated from the suspension by centrifugation, and the precipitation was twice repeated with 20 mL of acetone and 500 mL of hexane. The precipitate (4.5 g), dissolved in 10 mL of methanol–water mixture (7:3, V/V), was loaded on a polyamide column (15 g, 50–160 μm). Elution was carried out with a methanol–water mixture (7:3, V/V), and 100 mL fractions were collected. Fractions 3–8 were combined and evaporated until dry (2.5 g), then chromatographed on a silica-gel column (80 g, 40–63 μm). Three 150 mL fractions were eluted with the acetone–hexane mixture (5:4, V/V). The third fraction was evaporated until dry, and the residue (1.5 g) was finally purified by semi-preparative HPLC under the following conditions: C_{18} column (250×8 mm, 5 μm), acetonitrile–water mobile phase (0–11 min, 47% acetonitrile; 11–12 min, 47–90% acetonitrile; 12–15 min, 90% acetonitrile), with a flowrate of 3.0 mL min^{-1}, and detection at 280 nm. Fractions were collected as a single peak with Rt = 8.5–10.5 min, to obtain 1.15 g of nostotrebin 6.

Structure analysis of nostotrebin 6

The IR spectra were recorded on a Bruker Tensor 27 infrared spectrometer, in a KBr pellet. The NMR spectra were measured on a Bruker Avance 600 spectrometer, and referenced to residual solvent ^1H and ^{13}C signals (δ_H 2.05, δ_C 29.8 for acetone-d_6). The X-ray diffraction was measured on an Oxford Diffraction Xcalibur diffractometer, with graphite-monochromated Cu*Kα* radiation (λ = 1.54184 Å) at 150 K using the φ and ω scan techniques. The HPLC/MS and MS/MS measurements were performed on an Agilent 1100 Series LC/MSD Trap. The high resolution mass spectra (HRMS) were measured on a Bruker Apex-Q FTMS (Fourier transform mass spectrometer).

Analytical solutions for enzyme kinetics

Acetylcholinesterase (500 U) was dissolved in phosphate buffer pH 7.0 to produce a 20 U mL^{-1} stock solution, and stored at −27°C. Before use, the enzymatic activity was adjusted to 0.26 U mL^{-1}. Acetylthiocholine iodide was dissolved in

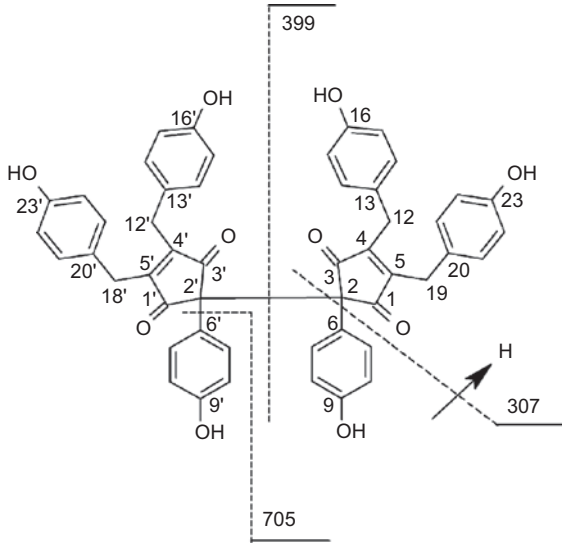

Figure 1. Chemical structure diagram of nostotrebin 6, shown together with the fragmentation scheme of the collision-induced dissociation of the molecular ion $[M + H]^+$ of nostotrebin 6.

RIGHTSLINK

Journal of Enzyme Inhibition and Medicinal Chemistry Downloaded from informahealthcare.com by University of South Carolina on 12/26/11
For personal use only.

phosphate buffer pH 8.0 in order to produce a 6.24 mM solution. Butyrylcholinesterase (1200 U) was dissolved in phosphate buffer pH 7.0 in order to produce a 24 U mL^{-1} stock solution, and stored at –27°C. Enzymatic activity was adjusted to 0.24 U mL^{-1} before use. Butyrylthiocholine iodide was dissolved in phosphate buffer pH 8.0 to produce a 5.67 mM solution. 5,5´-Dithiobis(2-nitrobenzoic acid) was dissolved in phosphate buffer pH 7.0 to make a 7.6 mM solution. All solutions were kept at 5°C. The acetylthiocholine iodide, BTCI, and DTNB solutions were freshly prepared each day.

Solutions of nostotrebin 6 (0.0–137.5 μM) were prepared in 50% methanol. Tacrine solutions (0.032–3.225 μM) were prepared in phosphate buffer pH 8.0. The galanthamine solutions (0.40 μM–1.03 mM) were prepared in demineralized water.

Acetylcholinesterase inhibition assay

The assay was carried out according to the Ellman method[12], optimized for 96-well microplates using a Tecan Sunrise™ absorbance reader. The initial reaction velocities were measured at different concentrations of the tested compound solution and fixed ATCI concentrations (0.062–1.25 mM). The reaction mixture contained 50 μL of 0.26 U mL^{-1} AChE, 25 μL of 7.6 mM DTNB, and 20 μL of the tested compound solution together with an aliquot volume of 6.24 mM ATCI solution in order to obtain the required concentration of ATCI in the final volume (250 μL) of reaction mixture, and 0.1 M phosphate buffer pH 8.0 in order to achieve the final volume of reaction mixture. For the blank, 50 μL of 0.26 U mL^{-1} AChE was replaced by the same volume of 0.1 M phosphate buffer pH 8.0. In a typical assay, solutions of AChE, DTNB, and the compound to be tested, as well as the phosphate buffer, were mixed and incubated for 30 min at 30°C. Next, the reaction was started by the addition of ATCI solution. The increase in absorbance at 412 nm was measured every 11 s for 220 s. Reaction velocities were determined from the slopes of the linear portions of the graphs of time versus concentration of 5-thio-2-nitrobenzoate. All assays were done in triplicate.

Butyrylcholinesterase inhibition assay

The BChE inhibition assay was carried out in the same manner as the AChE inhibition assay; however, the 0.26 U mL^{-1} of AChE was replaced by 0.24 U mL^{-1} of BChE, and the initial reaction velocities were measured at different BTCI concentrations (0.16–2.27 mM).

Results

Structure determination of nostotrebin 6

Nostotrebin 6 was isolated as a yellow powder at a yield of 1.7% (1.15 g) and with a purity of 99.8% (HPLC/MS). The crystal, suitable for X-ray analysis (with dimensions of 0.43 × 0.07 × 0.05 mm), was grown by slow cooling of the hot solution in methanol–water. Nostotrebin 6 crystallized in the orthorhombic crystal system, $P2_12_12$ space group, with the following cell parameters: a = 9.6453 (2) Å, b = 17.0686 (5) Å, c = 11.2313 (3) Å, V = 1849.03 (8) Å^3, Z = 2, D_x = 1.435 g cm^{-3}, and F_{000} = 836. X-ray crystallographic analysis of the nostotrebin 6 led to the determination of its structure as *meso*-2,2´-bis[4,5-bis(4-hydroxybenzyl)-2-(4-hydroxyphenyl) cyclopent-4-en-1,3-dione] with the molecular formula of $C_{50}H_{38}O_{10}$. The molecular conformation is stabilized by both intramolecular C–H…O hydrogen bonds, with two very short contacts (2.26 and 2.21 Å), as well as by the stacking interactions of the phenolic fragments (Figure 2). The structure of nostotrebin 6 was further supported by the NMR, MS, and IR measurements.

Signals of ^{1}H and ^{13}C NMR spectra of nostotrebin 6 (presented below) are in good agreement with the structure of nostotrebin 6, as determined by X-ray crystallography. The HRESIMS (high resolution electrospray ionization MS) spectrum of nostotrebin 6 showed a molecular peak $[M + H]^+$ *m/z* 799.2537, which correlates to the calculated value of 799.2543 for $C_{50}H_{39}O_{10}$. The collision-induced dissociation of the molecular peak $[M + H]^+$ resulted in three main fragment ions: $[M - C_{31}H_{23}O_6]^+$ *m/z* 307.1 (rel. int. = 63.0%), $[M - C_{25}H_{19}O_5]^+$ *m/z* 399.1 (rel. int. = 100.0%), and $[M - C_6H_5O]^+$ *m/z* 705.2 (rel. int. = 51.7%). The value of *m/z* 705.2 corresponds to the loss of the *p*-hydroxyphenyl group from the cyclopentenedionyl ring of $[M + H]^+$. Cleavage of the moiety, 4,5-bis(4-hydroxybenzyl)-2-(4-hydroxyphenyl) cyclo-pent-4-en-1,3-dione, as well as the loss of this moiety together with the *p*-hydroxyphenyl group, conforms with the daughter ions at *m/z* 399.1 and *m/z* 307.1, respectively. Fragmentation of nostotrebin 6 by collision-induced dissociation of the molecular peak $[M + H]^+$ is shown in Figure 1.

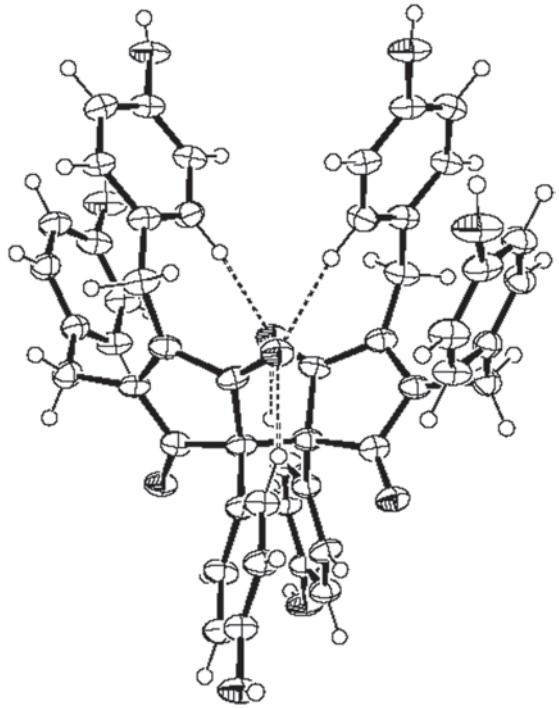

Figure 2. Molecular structure of nostotrebin 6 with the C–H…O intramolecular hydrogen bonds shown (dashed lines). The stacking interactions between phenolic fragments are also shown.

RIGHTSLINK

Journal of Enzyme Inhibition and Medicinal Chemistry Downloaded from informahealthcare.com by University of South Carolina on 12/26/11
For personal use only.

The IR spectrum showed strong bands assignable to the -OH (3416 cm^{-1}) and C=O (1690 cm^{-1}, 1230 cm^{-1}) groups. The strong band at 1690 cm^{-1} correlates to a five-membered cyclic (di)ketone. This value is decreased, due to the conjugation of a carbonyl group with an alkenyl C=C bond. Similarly, absorption at 1611 cm^{-1} indicates the presence of a C=C bond (sp^2), in conjugation with the C=O of the carbonyl group.

Nostotrebin 6 Yellowish needles (MeOH-H_2O), mp = 205–207°C; IR (KBr) ν_{max} 3416, 1735, 1690, 1611, 1512, 1439, 1349, 1230, 1016, 880 cm^{-1}; ^{1}H NMR (acetone-d_6, 600 MHz) δ 3.62 (4H, *bd*, J_{gem} = 14.0 Hz, H-12, H-19), 3.65 (4H, *bd*, J_{gem} = 14.0 Hz, H-12´, H-19´), 6.57 (4H, *m*, H-8, H-10), 6.63 (8H, *m*, H-15, H-17, H-22, H-24), 6.68 (4H, *m*, H-7, H-11), 6.85 (8H, *m*, H-14, H-18, H-21, H-25), 8.22 (4H, *br*, H4O, H5O), 8.46 (2H, *br*, H2O); ^{13}C NMR (acetone-d_6, 150 MHz) δ 29.1 ($4CH_2$, C-12, C-19), 59.4 (2C, C-2), 114.7 (4CH, C-8, C-10), 116.0 (8CH, C-15, C-17, C-22, C-24), 122.2 (2C, C-6), 128.1 (4C, C-13, C-20), 130.6 (8CH, C-14, C-18, C-21, C-25), 132.3 (4CH, C-7, C-11), 155.8 (4C, *b*, C-4, C-5), 156.8 (4C, C-16, C-23), 158.1 (2C, C-9), 201.0 (4C, *b*, C-1, C-3); ESIMS *m/z* (rel. int. %) 821.1 $[M + Na]^+$ (7), 799.4 $[M + H]^+$ (100), 399.1 (1); HRESIMS *m/z* 799.2537 (calcd. for $C_{50}H_{39}O_{10}$, 799.2543); ESIMS[2] $[M + H]^+$ *m/z* (rel. int. %) 705.2 (51.7), 399.1 (100.0), 307.1 (63.0).

Kinetic study

Nostotrebin 6 is a noncompetitive inhibitor of AChE, as shown in the Lineweaver–Burk plot (Figure 3). However, replots of the slope ($K_{m\ app}/V_{app}$) and 1/v-axis intercept ($1/V_{app}$) vs. [nostotrebin 6], constructed from the data of the Lineweaver–Burk plot, are both parabolic (Figure 4A), which is typical for the interaction of more than one molecule of the inhibitor with an enzyme. Moreover, dependence of $1/K_{i\ slope}$ vs. [nostotrebin 6] (Figure 4B), where the values of $1/K_{i\ slope}$ were calculated from the slopes of double reciprocal plots, is also a convex function. Figure 4C shows the Hill plot of dependence log $v_i/(v_0 - v_i)$ vs. log [nostotrebin 6] for 1.25 mM ATCI, with limiting slopes of –1.3 and –4.0. These values indicate that up to four molecules of nostotrebin 6 can bind to AChE. No cooperative binding was observed because the v vs. concentration of nostotrebin 6 gave a sigmoidal curve (Figure 4D). The IC_{50} value of AChE inhibition was determined from the Dixon plots (not shown) to be 5.5 μM for nostotrebin 6. The IC_{50} of galanthamine and tacrine were lower by about 10-fold and 100-fold, respectively. Table 1 summarizes the IC_{50} values of AChE inhibition together with the IC_{50} values of BChE inhibition and BChE/AChE selectivity, which were determined for nostotrebin 6 plus the reference standards galanthamine and tacrine.

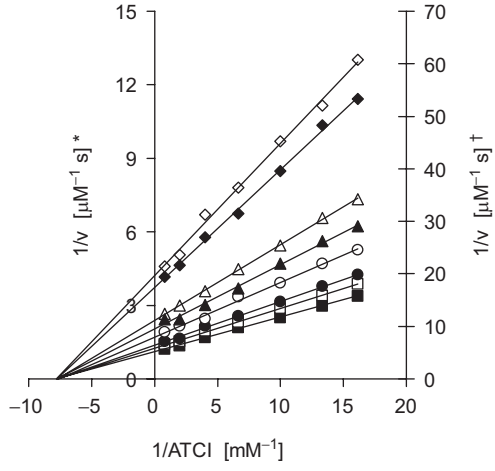

Figure 3. Lineweaver–Burk plot of AChE activity in the absence (■) and in the presence of nostotrebin 6 at different concentrations: 2.25 μM (□), 3.38 μM (●), 4.50 μM (○), 5.64 μM (▲), 6.76 μM (△), 9.00 μM (◆), and 11.00 μM (◊).

In the case of BChE, nostotrebin 6 was found to be a parabolic mixed-type inhibitor. The curves of the control and nostotrebin 6 (0.0–11.0 μM) intersect in the fourth quadrant of the Lineweaver–Burk plot (Figure 5). Further, the replots of the slope ($K_{m\ app}/V_{app}$) and 1/v-axis intercept ($1/V_{app}$) vs. [nostotrebin 6], constructed from the data of the Lineweaver–Burk plot, are both parabolic (Figure 6A). Dependence of $1/K_{i\ slope}$ vs. [nostotrebin 6] is also nonlinear (Figure 6B), and thus indicates more than two inhibitor-binding sites. The Hill plot for 0.908 mM BTCI is shown in Figure 6C. Its limiting slopes of –1.0 and –2.9 are suggestive of up to three binding sites of BChE for nostotrebin 6. Moreover, the linear dependence of v vs. [nostotrebin 6] indicates the cooperative binding of nostotrebin 6 to BChE (Figure 6D). The IC_{50} values of BChE inhibition by nostotrebin 6 were determined from Dixon plots (not shown) to be 6.1–7.5 μM (for a BTCI concentration range of 0.16–2.27 mM). The IC_{50} values of BChE inhibition by nostotrebin 6, as well as those of galanthamine and tacrine (as reference standards), are summarized in Table 1.

Discussion

The search for natural sources of new ChE inhibitors, especially AChE inhibitors that are useful in the treatment of Alzheimer's disease, have thus far been mainly focused on higher plants. Based upon our previous screening of autotrophic microorganisms, we isolated this new cholinesterase inhibitor nostotrebin 6 from the cyanobacteria *N.* sp. str. Lukešová 27/97.

The structure of nostotrebin 6, determined using a variety of methods (X-ray diffraction, NMR, IR, HRMS, and MS/MS), is unique, due to its 2,2´-bis(cyclopentenedione) skeleton with its cyclopentene double bond substituted by two *p*-hydroxybenzyl groups. In contrast, the currently known, naturally occurring cyclopentenediones are often either mono- or di-substituted on the double bond of the cyclopentenyl ring, and then only by methoxy or methyl groups[13–15]. Both the biosynthetic pathway of nostotrebin 6, and its biological function within *N.* sp. str. Lukešová 27/97, are unknown.

RIGHTSLINK

Journal of Enzyme Inhibition and Medicinal Chemistry Downloaded from informahealthcare.com by University of South Carolina on 12/26/11
For personal use only.

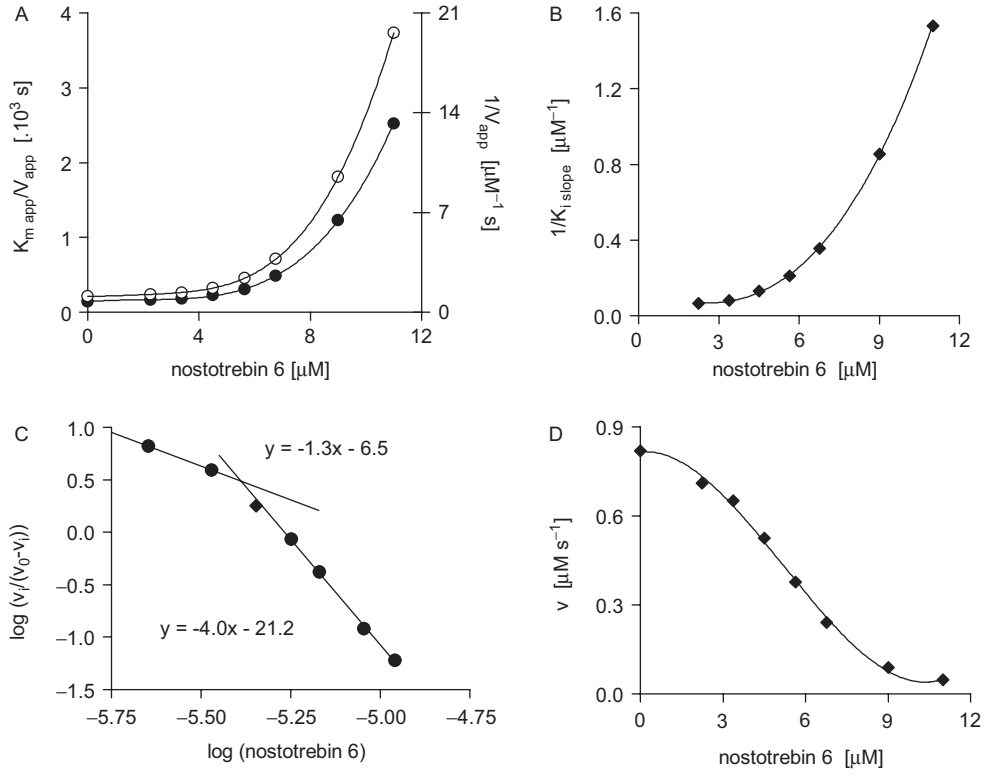

Figure 4. Analysis of the multiple inhibition of AChE by nostotrebin 6. (A) Replots constructed from data of the Lineweaver–Burk plot, as described in Figure 3: (●) $K_{m\,app}/V_{app}$ vs. [nostotrebin 6], (○) $1/V_{app}$ vs. [nostotrebin 6]. (B) Dependence of $1/K_{i\,slope}$ vs. [nostotrebin 6]. (C) Hill plot for AChE inhibition by nostotrebin 6 in the presence of 1.25 mM ATCI. (D) Dependence of v vs. [nostotrebin 6] for the hydrolysis of 1.25 mM ATCI by AChE.

Table 1. Cholinesterase inhibitory effects of nostotrebin 6, galanthamine, and tacrine *in vitro*.

Inhibitor	IC_{50} (μM)		Selectivity BChE/AChE
	AChE	BChE	
Nostotrebin 6	5.5	6.1–7.5[b]	1.4
Galanthamine	0.3–0.5[a]	8.6–37.9[b]	70.2
Tacrine	0.057	0.0062–0.012[b]	0.2

[a]For ATCI substrate range of 0.062–1.25 mM.
[b]For BTCI substrate range of 0.16–2.27 mM.

The biological activity of nostotrebin 6 was tested against both AChE from the electric eel and BChE from equine serum. It was further compared with the known ChE inhibitors tacrine and galanthamine.

Bioactive compounds are not only interesting candidates for new pharmaceuticals, but they are also important in ecotoxicology. Cyanobacteria are generally known for their production of various toxins, e.g. microcystins, nodularins, and saxitoxins[16]. Cyanotoxins, which are responsible for organism intoxications, usually occur in water bodies (both within and between blooms). However, *N.* sp. str. Lukešová 27/97, which produces nostotrebin 6, is a soil cyanobacterium, therefore having no assumption of excessive growth combined with the high production of nostotrebin 6.

Nostotrebin 6 has been found to be an *S*-parabolic *I*-parabolic noncompetitive inhibitor of AChE, and an *S*-parabolic *I*-parabolic mixed-type inhibitor of BChE. Therefore, the inhibition constants K_i cannot be determined

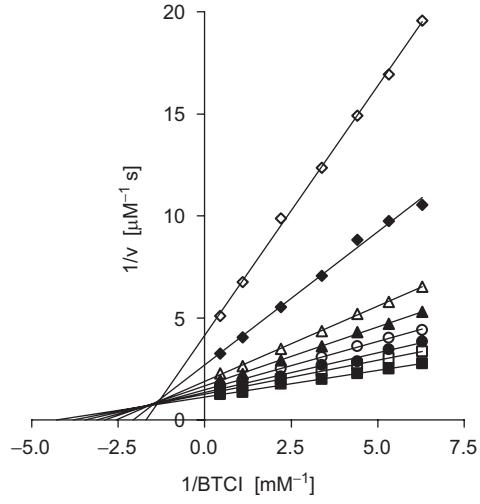

Figure 5. Lineweaver–Burk plot of BChE activity in the absence (■) and in the presence of nostotrebin 6 at different concentrations: 2.25 μM (□), 3.38 μM (●), 4.50 μM (○), 5.64 μM (▲), 6.76 μM (△), 9.00 μM (◆), and 11.00 μM (◊).

directly from the Lineweaver–Burk plots (or replots of the Lineweaver–Burk plots or Dixon plots, in these cases). If an enzyme possesses two inhibitor-binding sites, the K_i can be obtained from the linear dependence of $1/K_{i\,slope}$ vs. inhibitor concentration. However, the convex shape of the $1/K_{i\,slope}$ vs. [nostotrebin 6] makes the K_i determination impossible, and indicates more than two binding sites[17].

RIGHTSLINK

Journal of Enzyme Inhibition and Medicinal Chemistry Downloaded from informahealthcare.com by University of South Carolina on 12/26/11
For personal use only.

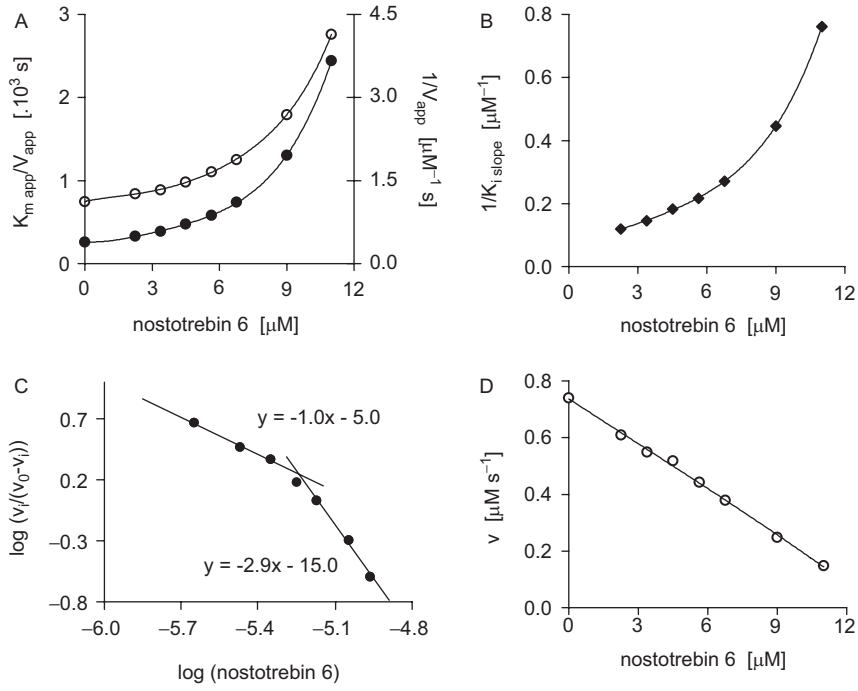

Figure 6. Analysis of the multiple inhibition of BChE by nostotrebin 6. (A) Replots constructed from data of the Lineweaver–Burk plot, as described in Figure 5: (●) $K_{m\ app}/V_{app}$ vs. [nostotrebin 6], (○) $1/V_{app}$ vs. [nostotrebin 6]. (B) Dependence of $1/K_{i\ slope}$ vs. [nostotrebin 6]. (C) Hill plot for BChE inhibition by nostotrebin 6 in the presence of 0.908 mM BTCI. (D) Dependence of v vs. [nostotrebin 6] for the hydrolysis of 0.908 mM BTCI by BChE.

Analysis of the Hill plots confirmed multiple binding sites for nostotrebin 6 on both AChE and BChE. The binding of a single inhibitor molecule to an enzyme in multiple inhibition either can (with cooperative binding) or cannot (with non-cooperative binding) affect the intrinsic dissociation constant K_i of the vacant inhibitor sites. Non-cooperative binding (without changes in the intrinsic K_i) can be distinguished from cooperative binding using the dependence of the reaction velocity (v) vs. the inhibitor concentration. Nostotrebin 6 displayed cooperative binding to BChE; however, because there was no determination of cooperative binding to AChE, the random and independent binding of nostotrebin 6 to AChE can be assumed.

In compliance with the determined structure of nostotrebin 6, π–π interactions among both the *p*-hydroxyphenyl and *p*-hydroxybenzyl groups of nostotrebin 6, and the side chains of the aromatic amino acids of AChE, should participate in the affinity between nostotrebin 6 and AChE. Hydrogen bonds are another type of interaction that should be expected in the nostotrebin 6 and AChE complex; this is due to the presence of hydroxy and keto groups in the nostotrebin 6 molecule. Similar noncovalent interactions should also participate in the affinity of nostotrebin 6 to BChE.

Currently, all of the ChE inhibitors known to be produced by autotrophic microorganisms only constitute a tiny percentage of the total known (compared to the numbers found in higher plants). Nostocarboline, a quaternary β-carboline alkaloid produced by the cyanobacterium *Nostoc* 78-12A, inhibits both AChE (IC_{50} = 5.3 μM) and BChE (IC_{50} = 13.2 μM)[7,8]. *Ecklonia stolonifera* Okamura is a producer of several ChE inhibitors, belonging to the sterol and phlorotannin groups[9]. The most active is the phlorotannin (named phlorofucofuroeckol-A), a reversible inhibitor of both AChE (IC_{50} = 4.98 μM) and BChE (IC_{50} = 136.71 μM). Accordingly, the inhibitory activity of nostotrebin 6 on ChE is comparable to the strongest reversible ChE inhibitors isolated from autotrophic microorganisms. Nostotrebin 6 is also a relatively high-potency ChE inhibitor, compared to substances isolated from higher plants, which usually demonstrate an IC_{50} in the range from several units to hundreds of micromoles. However, the reference standards galanthamine and tacrine are much stronger AChE inhibitors. Only BChE is a bit more strongly inhibited by nostotrebin 6 than it is by galanthamine. Therefore, it is unlikely that nostotrebin 6 could compete with those pharmaceuticals currently used in AD therapy.

Appendix

Crystallographic data for the structure reported in this article have been deposited with the Cambridge Crystallographic Data Centre. A copy of the data can be obtained, free of charge, on application to the Director, CCDC 706268, 12 Union Road, Cambridge CB2 1EZ, UK (fax: +44-(0)1223-336033 or e-mail: deposit@ccdc.cam.ac.uk).

Declaration of interest:
This research was supported by Project ME 874 of the Ministry of Education, Youth, and Sports of the Czech Republic. The Czech Science Foundation further supported

RIGHTSLINK

this work through Project 522/06/1090. Partial funding was also provided by Project MSM6007665808 of the Ministry of Education, Youth, and Sports of the Czech Republic, and also by Projects AVOZ 50200510 and AVOZ 6060521 of the Czech Academy of Sciences.

References

1. Vinters H, Felix J. The neuropsychiatry of Alzheimer's disease and related dementias. In: Cummings JL, ed. Alzheimer's Disease. London: Martin Dunitz, 2003:57–116.
2. Ballard CG. Advance in the treatment of Alzheimer's disease: benefits of dual cholinesterase inhibition. Eur Neurol 2002;47:64–70.
3. Shimizu Y. Microalgal metabolites: a new perspective. Annu Rev Microbiol 1996;50:431–65.
4. Monserrat JM, Yunes JS, Bianchini A. Effect of *Anabaena spiroides* (Cyanobacteria) aqueous extracts on the acetylcholinesterase activity of aquatic species. Environ Toxicol Chem 2001;20:1228–35.
5. Stirk WA, Reinecke DL, Staden J. Seasonal variation in antifungal, antibacterial and acetylcholinesterase activity in seven South African seaweeds. J Appl Phycol 2007;19:271–6.
6. Mahmood NA, Carmichael WW. Anatoxin-a(s), an anticholinesterase from the cyanobacterium *Anabaena flos-aquae* NRC-525-17. Toxicon 1987;25:1221–7.
7. Becher PG, Beuchat J, Gademann K, Jüttner F. Nostocarboline: isolation and synthesis of a new cholinesterase inhibitor from *Nostoc* 78-12A. J Nat Prod 2005;68:1793–5.
8. Becher PG, Baumann HI, Gademann K, Jüttner F. The cyanobacterial alkaloid nostocarboline: an inhibitor of acetylcholinesterase and trypsin. J Appl Phycol 2009;21:103–10.
9. Yoon NY, Chung HY, Kim HR, Choi JS. Acetyl- and butyrylcholinesterase inhibitory activities of sterols and phlorotannins from *Ecklonia stolonifera*. Fish Sci 2008;74:200–7.
10. Zelík P, Lukešová A, Voloshko LN, Štys D, Kopecký J. Screening for acetylcholinesterase inhibitory activity in cyanobacteria of the genus *Nostoc*. J Enzyme Inhib Med Chem 2009;24:531–6.
11. Allen MB, Arnon DI. Studies on nitrogen-fixing blue green algae: I. Growth and nitrogen fixation by *Anabaena cylindrica* Lemm. Plant Physiol 1955;30:366–72.
12. Ellman GL, Courtney KD, Andres V, Featherstone RM. A new rapid colorimetric determination of acetylcholinesterase activity. Biochem Pharmacol 1961;7:88–95.
13. Oh H-M, Choi S-K, Lee JM, Lee S-K, Kim H-Y, Han DC, et al. Cyclopentenediones, inhibitors of farnesyl protein transferase and anti-tumor compounds, isolated from the fruit of *Lindera erythrocarpa* Makino. Bioorg Med Chem 2005;13:6182–7.
14. Gilardoni G, Clericuzio M, Tosi S, Zanoni G, Vidari G. Antifungal acylcyclopentenediones from fruiting bodies of *Hygrophorus chrysodon*. J Nat Prod 2007;70:137–9.
15. Facundo VA, Sá AL, Silva SAF, Morais SM, Matos CRR, Braz-Filho R. Three new natural cyclopentenedione derivates from *Piper carniconnectivum*. J Braz Chem Soc 2004;15:140–5.
16. Apeldoorn ME, Egmond HP, Speijers GJA, Bakker GJI. Toxins of cyanobacteria. Mol Nutr Food Res 2007;51:7–60.
17. Segel IH. Enzyme Kinetics. Behavior and Analysis of Rapid Equilibrium and Steady-State Enzyme Systems. New York: John Wiley & Sons, 1975:463–70.

Journal of Enzyme Inhibition and Medicinal Chemistry Downloaded from informahealthcare.com by University of South Carolina on 12/26/11
For personal use only.

RIGHTSLINK